Molecular determinants of acidic pH-dependent transport of human equilibrative nucleoside transporter 3

Received for publication, March 22, 2017, and in revised form, July 11, 2017 Published, Papers in Press, July 20, 2017, DOI 10.1074/jbc.M117.787952

Md Fazlur Rahman[‡], **Candice Askwith**[§], **and Rajgopal Govindarajan**[‡¶1]

From the [‡]*Division of Pharmaceutics and Pharmaceutical Chemistry, College of Pharmacy, the* [§]*Department of Neuroscience, and the* [¶]*Translational Therapeutics Program, Ohio State University Comprehensive Cancer Center, Ohio State University, Columbus, Ohio 43210*

Edited by Thomas Söllner

Equilibrative nucleoside transporters (ENTs) translocate hydrophilic nucleosides across cellular membranes and are essential for salvage nucleotide synthesis and purinergic signaling. Unlike the prototypic human ENT members hENT1 and hENT2, which mediate plasma membrane nucleoside transport at pH 7.4, hENT3 is an acidic pH-activated lysosomal transporter partially localized to mitochondria. Recent studies demonstrate that hENT3 is indispensable for lysosomal homeostasis, and that mutations in hENT3 can result in a spectrum of lysosomal storage-like disorders. However, despite hENT3's prominent role in lysosome pathophysiology, the molecular basis of hENT3-mediated transport is unknown. Therefore, we sought to examine the mechanistic basis of acidic pH-driven hENT3 nucleoside transport with site-directed mutagenesis, homology modeling, and [^{3}H]adenosine flux measurements in mutant RNA-injected *Xenopus* oocytes. Scanning mutagenesis of putative residues responsible for pH-dependent transport via hENT3 revealed that the ionization states of Asp-219 and Glu-447, and not His, strongly determined the pH-dependent transport permissible-impermissible states of the transporter. Except for substitution with certain isosteric and polar residues, substitution of either Asp-219 or Glu-447 with any other residues resulted in robust activity that was pH-independent. Dual substitution of Asp-219 and Glu-447 to Ala sustained pH-independent activity over a broad range of physiological pH (pH 5.5–7.4), which also maintained stringent substrate selectivity toward endogenous nucleosides and clinically used nucleoside drugs. Our results suggest a putative pH-sensing role for Asp-219 and Glu-447 in hENT3 and that the size, ionization state, or electronegative polarity at these positions is crucial for obligate acidic pH-dependent activity.

Two human nucleoside transporter gene families encoding the human concentrative nucleoside transporters (SLC28; hCNTs)[2] and equilibrative nucleoside transporters (SLC29; hENTs) are required for the membrane transport of hydrophilic nucleosides (1–4). hCNTs are unidirectional, Na^+-driven, high-affinity transporters with a defined substrate selectivity (2, 4), *i.e.* hCNT1 transports pyrimidine nucleosides, hCNT2 transports purine nucleosides, and hCNT3 transports both nucleosides. hENTs are bidirectional, Na^+-independent, high-capacity transporters with a wider substrate selectivity (1, 3), *i.e.* all hENTs transport both purine and pyrimidine nucleosides with some ENTs even transporting nucleobases (ENT2 and ENT3), nucleotides (ENT3), and cyclic nucleotides (ENT2) (1, 3). Expression of hCNTs is largely restricted to differentiated epithelial tissues, *e.g.* liver, kidney, brain, and intestine (5–9), whereas hENTs are expressed ubiquitously (1, 3, 10). Studies to date suggest that both hCNTs and hENTs are essential for the salvage synthesis of nucleotides and purinergic signaling and determining the clinical efficacy of therapeutic nucleoside drugs (1–4).

In the past decade considerable knowledge has been gained into understanding the molecular determinants of hCNT transport particularly with respect to nucleoside and sodium binding (11–13), and recently, the crystal structure of a CNT from *Vibrio cholerae* was elucidated (14). However, hENTs are predominantly evaluated for functional roles using *in vitro* systems (*e.g. Xenopus* oocytes, lipid vesicles, and cultured cells) and mouse models with limited knowledge available on the structural basis of transport (1, 3). Although site-directed mutagenesis studies and chimeric ENT analysis are beginning to identify specific transmembrane regions and residues involved in the substrate selectivity (endogenous nucleosides and therapeutic nucleoside analogs) and inhibitor (*e.g.* cardiovascular drugs)-binding characteristics of ENTs (15–17), no crystal structures are available for any member of this family. Because hENTs and hCNTs are structurally unrelated and differ in the number of predicted transmembrane domains (11 *versus* 13), transport directionalities (bidirectional *versus* unidirectional), and cotransport (none *versus* sodium) requirements, it makes extrapolation of hCNT structural information to hENTs difficult. Furthermore, all hENTs (hENT1, -2, -3, and

This work was supported, in whole or in part, by National Institutes of Health Grants R03AR063326 (to R. G.) and R01CA188464 (to R. G.). The authors declare that they have no conflicts of interest with the contents of this article. The content is solely the responsibility of the authors and does not necessarily represent the official views of the National Institutes of Health.
This article contains supplemental Table S1 and Figs. S1–S4.

[1] To whom correspondence should be addressed: Pharmaceutics and Pharmaceutical Chemistry, College of Pharmacy, Ohio State University, 542 Riffe Bldg., 12th Ave., Columbus, OH 43210. Tel.: 614-247-8269; Fax: 614-292-2588; E-mail: govindarajan.21@osu.edu.

[2] The abbreviations used are: (h)CNT, (human) concentrative nucleoside transporter; hENT, (human) equilibrative nucleoside transporter; PHID, pigmented hypertrichosis with insulin-dependent diabetes mellitus syndrome; SHML, sinus histiocytosis with massive lymphadenopathy; RDD, Rosai-Dorfman disease.

-4) have a very similar membrane topology as well as substrate and inhibitor-binding characteristics (1, 3), yet individual hENTs drastically differ in their functional activity at various physiological pH as well as their cellular and subcellular distributions. In this regard, hENT1 and hENT2 function at pH 7.4, hENT3 functions at pH 5.5, and hENT4 functions at pH 5.5–6.5 (10, 18). Consistent with their apparent transport maxima, hENT1 and hENT2 are primarily localized to the cell surface (1, 3), whereas hENT3 is localized to vesicular and tubular intracellular organelles including the late endosome/lysosome and mitochondria (10, 19). hENT4 is found in the plasma membrane of ventricular myocytes and vascular endothelial cells and transports adenosine in an acidic pH-dependent manner. However, hENT4 has been renamed as the plasma membrane monoamine transporter due to its relatively higher affinity to monoamines (*e.g.* serotonin) than adenosine (18).

Recently, numerous reports from independent laboratories have identified exclusive mutations in hENT3 that cause a wide range of human clinical disorders (H syndrome, PHID (pigmented hypertrichosis with insulin-dependent diabetes mellitus syndrome) syndrome, SHML (sinus histiocytosis with massive lymphadenopathy)/RDD (Rosai-Dorfman Disease) syndrome, dysosteosclerosis, etc.) with intriguing resemblances to lysosome storage-like and mitochondrial disorders (20–31). However, the precise mechanism of disease pathogeneses and possible treatment interventions for these disorders is not understood largely due to a lack of information on the hENT3 structural and functional characteristics. We undertook this project to determine the mechanistic basis of acidic pH-dependent activity of hENT3 to better understand the subcellular transport characteristics of nucleosides. Here, we report the ionization states of Asp-219 and Glu-447 in hENT3 to determine the pH-dependent transport permissible-impermissible conformational states of the transporter by acting as pH sensors of the transport microenvironment.

Results

hENT3 is an acidic pH-activated, non-electrogenic nucleoside transporter

Transportability of hENT1 and -2 is generally tested at the physiological blood pH (pH 7.4), which is representative of the pH at the cell surface and within the interstitium. However, secondary localization in intracellular organelles is reported for many hENTs including hENT1 and hENT2, where the pH could vary significantly from pH 7.4 (10, 19, 32). Conversely, hENT3 is primarily identified intracellularly with partial localization in lysosomes and mitochondria (10, 19). To test the functionality of hENTs in a wide range of physiologically relevant pH values, [^{3}H]adenosine transport levels of hENT cRNA injected *Xenopus* oocytes were analyzed using extracellular solutions buffered between pH 4.5 and 8.5 (Fig. 1*A*). Surprisingly, the total flux of tritiated [^{3}H]adenosine of hENT1- or hENT2-injected oocytes was robust even at a low pH. In fact, transport was not significantly different throughout the entire pH range tested (pH 4.5 to pH 8.5) (Fig. 1*A*). To investigate transport of hENT3, we utilized the Δ36hENT3 construct in which the N-terminal 36 amino acids of hENT3 are deleted to enable cell-surface localization of an otherwise intracellular transporter (10, 20). Conversely to the results with hENT1 and hENT2, the [^{3}H]adenosine transport maxima of Δ36hENT3 was seen at pH 5.5 and was reduced drastically in transport solutions with pH values >6.5 (Fig. 1*A*). The transport maximum for hENT4 was observed at pH 5.5–6.5 as reported earlier (Fig. 1*A*) (18). The maximal flux of adenosine in oocytes varied significantly among hENTs, which is likely due to differences in affinities of hENTs to adenosine (K_m effect) and their expression levels on the oocyte cell surface (V_{max} effect) (Fig. 1*A*). To relate to the pH-dependent activities of hENTs, we utilized an R-value (defined as the ratio of the transport flux at pH 7.4 to that of at pH 5.5) as reported earlier for an *Escherichia coli* acidic pH-dependent arginine-agmatine antiporter (33). If the R value is close to 1, the transporter is completely pH independent, and if the R value is close to 0 the transporter is completely pH-dependent. The estimated R values (in parenthesis) for hENTs demonstrated a rank order of hENT3 (0.07) > hENT4 (0.63) > hENT2 (1.02) > hENT1 (1.02). This indicates that hENT3 is the strongest pH-dependent member of the family followed by hENT4, and hENT1 and hENT2 are pH-independent members (Fig. 1*B*).

Similar to hENT3, the mouse ortholog, mENT3, is also an acidic pH-driven transporter (10). However, the fungal ortholog of ENT3, Fun26, which localizes to acidic vacuoles analogous to lysosomes in mammals, was reported to be a pH-independent transporter (34). These findings suggested a possible functional divergence of the pH-dependent transport activity within the mammalian ENT families. In search of the amino acid changes responsible for this divergence, we performed sequence identity and similarity comparisons among the human, mouse, and rat ENT family members using Clustal Omega and constructed a phylogenetic tree using Genebee Services (Fig. 1*C*). These analyses showed hENT4 has the highest sequence identity (20.175) and similarity (165) with hENT3, the only other pH-sensitive member of the family (supplemental Fig. S1). The analysis also suggested that the amino acids conferring pH dependence would be conserved in more similar members (hENT3 and hENT4) than in distant (hENT1 and hENT2) members of SLC29 family (supplemental Fig. S2). Furthermore, the phylogenetic analysis showed that divergence of hENT4 from hENT1, -2, and -3 is the earliest event in the metazoan evolution that is followed by divergence of hENT3 from hENT1 and hENT2 in vertebrates (Fig. 1*C*).

Some acidic pH-dependent lysosomal transporters require proton co-transport with their substrates. In addition, the ENT family of transporters from kinetoplastid protozoa is also reported to be proton/nucleoside cotransporters (35). Whether hENT3 required proton cotransport for permeant translocation was unknown. To test this possibility, oocytes expressing were Δ36hENT3 were clamped at −50 mV, and adenosine was added at a 100 μM concentration to measure proton cotransport by electrophysiological measurements. Human CNT2 cRNA-injected oocytes were used as a positive control, and hCNT2-injected oocytes induced an inward current of −89.5 ± 13.5 nA consistent to its known Na^+-driven nucleoside transport activity (36, 37). However, Δ36hENT3 oocytes showed no detectable current with adenosine addition at pH 5.5 and dis-

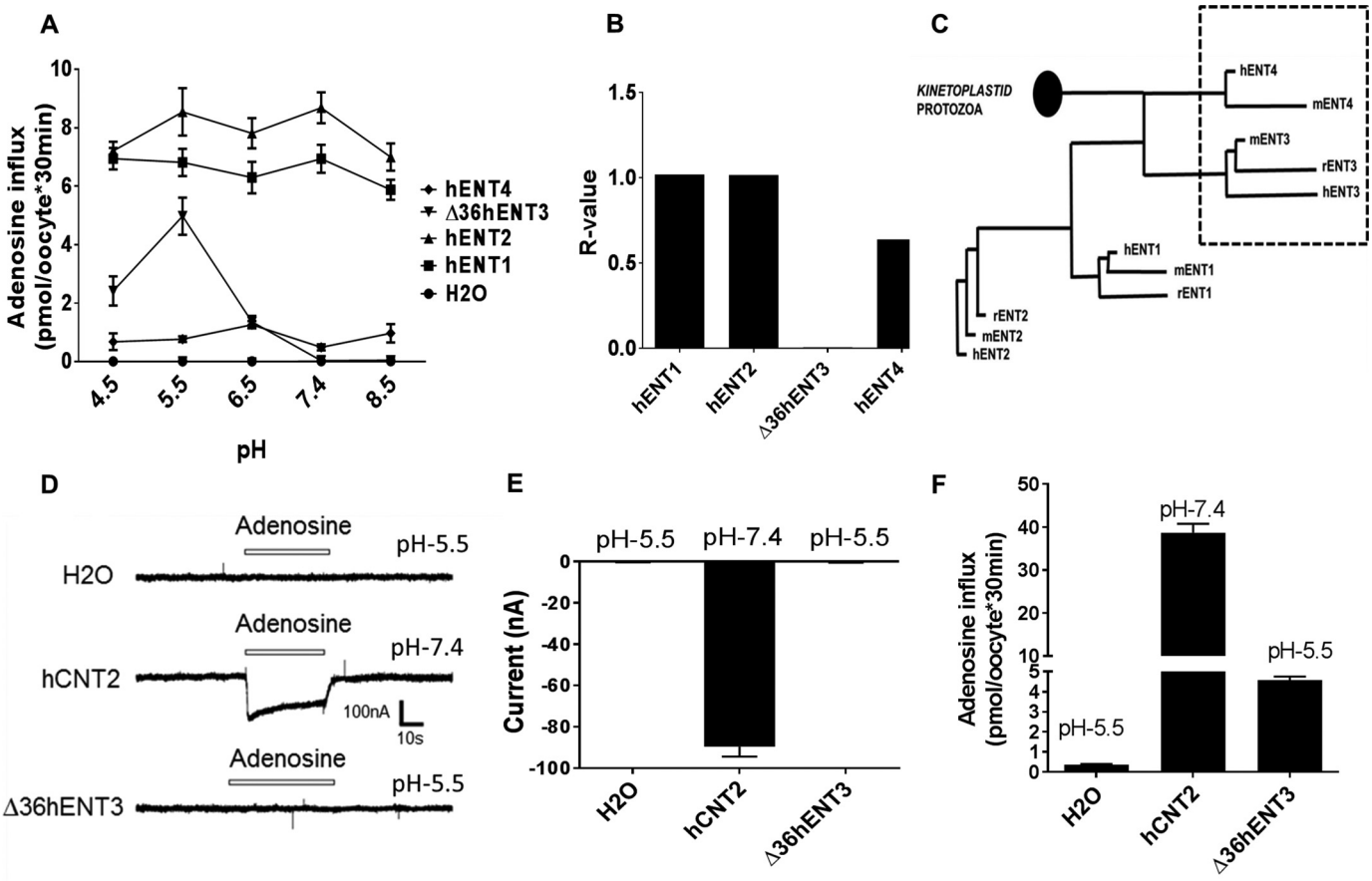

Figure 1. Analyses of the pH-dependent transport activity of hENT family members: hENT3 is an acidic-pH activated, non-electrogenic transporter. *A*, transport activities of H_2O, hENT1, hENT2, Δ36hENT3, and hENT4 transcripts injected *Xenopus* oocytes at a pH range 4.5–8.5. Uptake of [^{3}H]adenosine (20 μM) into oocytes at 25 °C after 22 h of injection of transcripts was measured in transport buffers with different pH. *B*, R value: the ratio of the ^{3}H-labeled adenosine uptakes by hENT1, hENT2, Δ36hENT3, and hENT4 at pH 7.4 to that at pH 5.5. *C*, phylogenetic analyses of pH dependence of human, mouse, and rat ENT family constructed from the sequences of human, mouse, and rat ENTs. Primary sequences were obtained from Uniprot and aligned using Clustal Omega. The phylogenetic tree was generated using Genebee pH-sensitive members are shown (*box*). *D*, representative traces of the electrophysiological analyses of adenosine administration on hCNT2-, Δ36hENT3-, and H_2O-injected oocytes. *E*, the average current values from 8–10 oocytes for H_2O, hCNT2, and Δ36hENT3. *F*, the transport activities of [^{3}H]adenosine (20 μM) by H_2O, hCNT2, and Δ36hENT3 transcripts-injected *Xenopus* oocytes (same batch of oocytes with the electrophysiological analyses oocytes) pH 5.5 and 7.4. Data show the average ± S.E. (n = 8–10 oocytes).

played electrophysiological activity similar to water-injected oocytes. These data identified hENT3 is an acidic-pH activated, non-electrogenic nucleoside transporter and indicate that proton transport is not concurrent to adenosine transport.

Histidine switches contribute minimally to pH-dependent activity of hENT3

Because Δ36hENT3 transport activity at pH 5.5 was not driven by protons, we hypothesized that the interactions between protons and amino acids in hENT3 could be important for its strictly acidic pH-activated transportability. In search for the amino acid residues responsible for pH dependence of hENT3, we conducted comprehensive site-directed mutagenesis studies. There are three groups of amino acids that could play a role in pH-sensing mechanisms as reported for other pH-driven bacterial and mammalian transporters (33). The first group includes the ionizable amino acids His, Asp, and Glu, which can be protonated or deprotonated within a physiological pH range (Fig. 2*A*). The second group encompasses aromatic amino acids Phe, Tyr, and Trp, whose side chains can sense the presence of protons by their π electrons (33, 38, 39) and can also act as anchors to stabilize transmembrane orientation for substrate recognition or transport (Fig. 2*A*). Ser, Thr, and Cys make up the third group as they have slightly basic pK_a values and can act as pH sensors under rare circumstances (33) (Fig. 2*A*).

Because the pK_a (~6.0) of the imidazole ring of His lies precisely between the transport-permissible (pH 5.5) and impermissible states (pH 7.4) of hENT3, we first investigated His residues as potential pH sensors. There are 6 His residues in hENT3 (at positions 11, 132, 268, 294, 403, and 473). Because Δ36hENT3 showed pH-dependent activity (10, 20), we omitted His at position 11 for analysis as it is not likely to act as a pH sensor. A His-less hENT3 mutant was created by replacing the remaining His residues with the non-ionizable amino acid Ala, and the ability of this mutant protein to transport [^{3}H]adenosine was assessed at pH 5.5 (Fig. 2*B*). The His-less Δ36hENT3 mutant completely lost its ability to transport [^{3}H]adenosine into oocytes at pH 5.5 and 7.4, identifying the possibility of one or more His amino acids playing a role in pH sensing. However, loss of transportability could have also occurred due to other general transportability attributes such as the loss of substrate

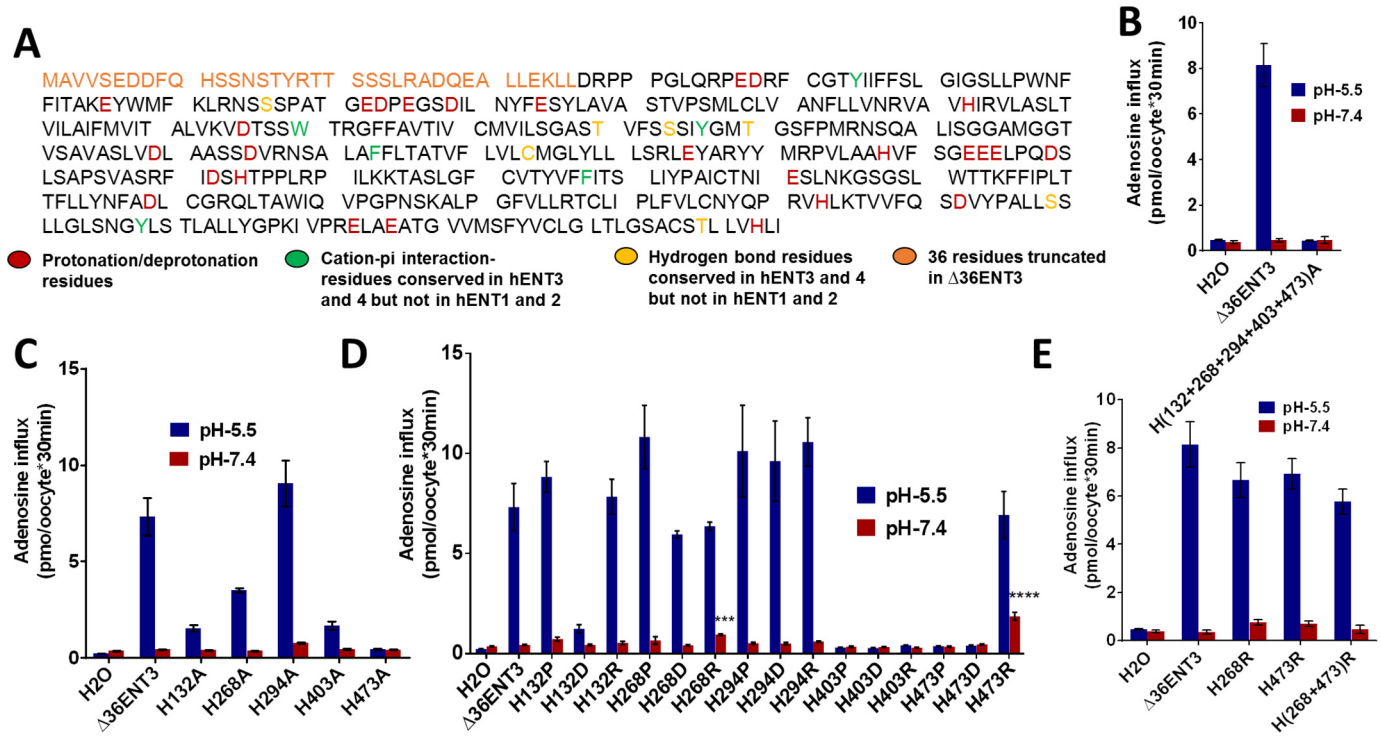

Figure 2. Histidine residues contributed minimally to pH-dependent activity of hENT3. *A*, primary sequence of hENT3 (Uniprot) is presented. Three categories of putative amino acids dictating pH sensitivity were investigated (*red*, *green*, *yellow*). *B*, adenosine (20 μM) transport activity analysis of His-less Δ36hENT3 mutant. *C*, individual His-to-Ala mutations in Δ36hENT3. *D*, Pro, Asp, and Glu substitution mutations of His in hENT3. *E*, His double mutants at pH 5.5 and 7.4. Data show the average ± S.E. (n = 15–18 oocytes). *, p 0.05; **, p 0.01; ***, p 0.005; ****, p 0.001 (one-way analysis of variance mutants compared with Δ36hENT3 at pH −7.4).

recognition, loss of binding interactions, and improper membrane targeting, etc.

To further delve into the pH-sensing mechanism of His in particular, we analyzed mutant transporters with His residues in Δ36hENT3 converted to either Ala or the non-ionizable, rigid amino acid Pro (both mimic uncharged His), negatively charged Asp (the side chain potentially stays negatively charged at pH-7.4 depending on surroundings), and positively charged Arg (the side chain potentially mimics protonated His at both pH 5.5 and 7.4) (Fig. 2, *C* and *D*). Our hypothesis was that if a particular His residue is a pH sensor, then the positively charged side chain of His at pH 5.5 would confer a transport-permissible state, and the neutral side chain at pH 7.4 would confer the transport-impermissible state. Ala or Pro replacements of His should then result in transport impermissible conformations at both pH 5.5 and 7.4. Similarly, Asp replacement should also result in a transport impermissible conformation at both pH 5.5 and 7.4. Arg replacement, however, should result in transportability at both pH 5.5 and 7.4. Transport measurements at pH 5.5 demonstrated substitutions of His to Ala at all positions except for 294 reduced or abolished [^{3}H]adenosine transport activity similar to that observed with Δ36hENT3 histidine-less mutant (Fig. 2*C*). Furthermore, at pH 5.5, replacement of His-132 with Pro and Arg fully recovered the functional activity of hENT3 that was lost with Ala substitution (Fig. 2*D*). Because none of the Pro-, Asp-, or Arg-substituted mutants at His-132 was functional at pH 7.4, our results excluded His at position 132 as a possible pH sensor (Fig. 2*D*). Pro, Asp, and Arg substitutions of His-294 were functional at pH 5.5 but not at pH 7.4, indicating His-294 did not contribute to pH-sensing activity (Fig. 2*D*). Pro, Asp, and Arg substitutions of His-403 were non-functional at both pH 5.5 and pH 7.4, suggesting His-403 contributes to general transportability of hENT3 but not to pH-sensing activity (Fig. 2*D*). Together, these findings eliminated His at positions 132, 294, and 403 as possible pH sensors.

Interestingly, when probed into the remaining two His (His-268 and His-473), we found the Pro substitution of His-268 restored the functional activity of hENT3 at pH 5.5 that was lost with the Ala substitution (Fig. 2*D*). Although Asp substitution of His-268 was functional at pH 5.5 and non-functional at pH 7.4, Arg substitution retained ~81% of the total transport activity at pH 5.5 and enabled ~2.2-fold higher transport activity than Δ36hENT3 at pH 7.4 (Fig. 2*D*). These data identified a positive charged residue at position 268 to play a role in pH-sensing. In the case of His at position 473, Pro and Asp substitutions were non-functional at pH 5.5 (similar to the H473A mutation), and Arg substitution of His-473 demonstrated functionality at both pH 5.5 (94% of Δ36hENT3) and 7.4 (4.2-fold higher than Δ36hENT3) (Fig. 2*D*). Together, these results suggested the positively charged residues at both the 268 and 473 positions contribute toward the acidic pH (pH 5.5)-activated transport of hENT3. However, the lack of robust recovery of transport activity in Arg-substituted mutants at pH 7.4 (only 2–4-fold; estimated R value of ~0.15 and ~0.26, respectively) argued against His-268 and His-473 as possible major pH sensors of hENT3. Furthermore, double mutations of His to Arg at positions 268 and 473 did not improve transportability any fur-

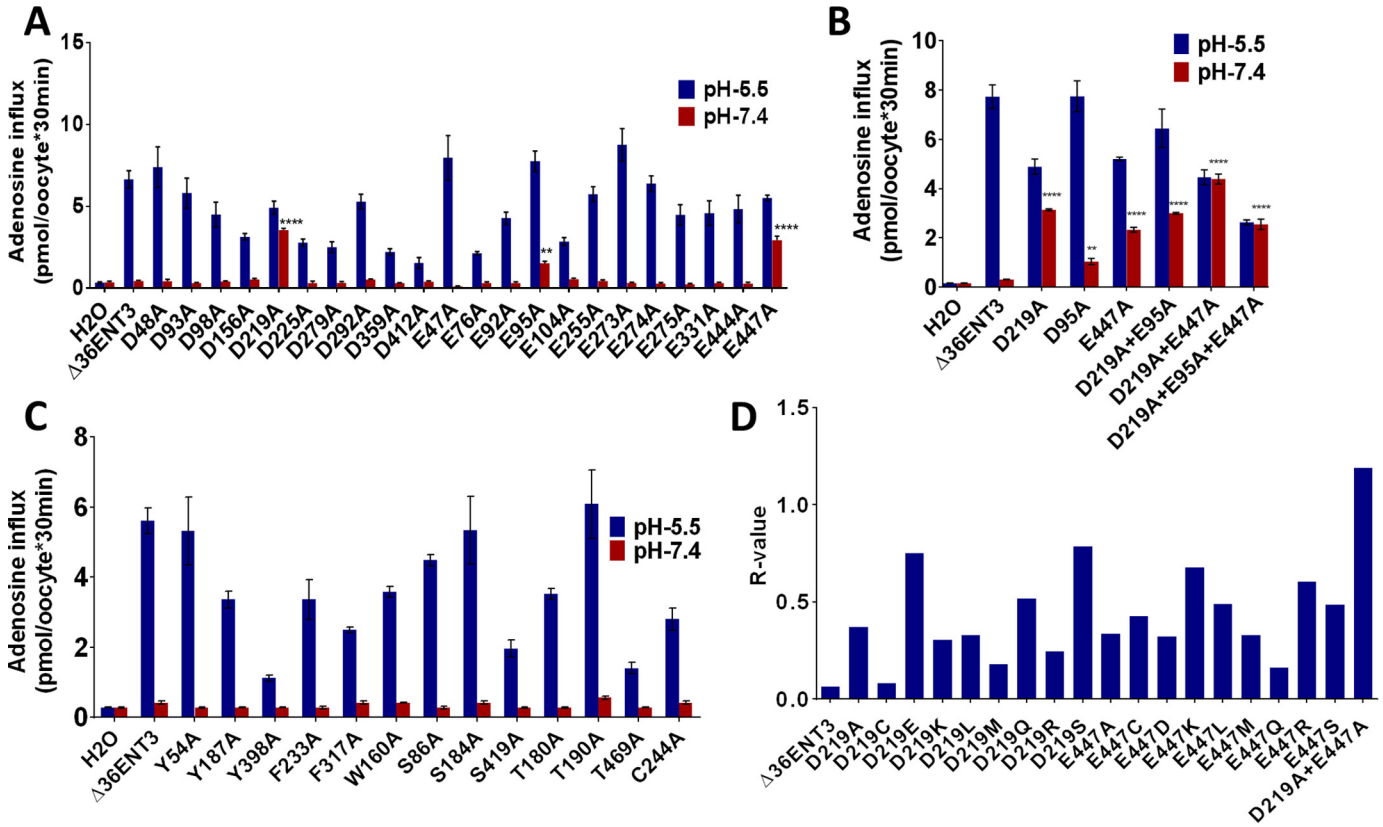

Figure 3. Scanning mutagenesis of Asp, Glu, and other potential residues contributing to pH-dependent activity of hENT3. *A*, adenosine (20 μM) transport activity analyses at pH 5.5 and pH 7.4 after Ala replacement of Asp and Glu residues. *B*, combination of mutations of residues dictating pH sensitivity. *C*, transport activity analyses after Ala replacement of Tyr, Phe, Trp, Ser, Thr, and Cys residues. *D*, R values derived from transport analysis after scanning mutagenesis of residues Asp-219 and Glu-447 in hENT3. Data show the average ± S.E. (n = 15–18 oocytes). **, p 0.01; ****, p 0.001 (one way analysis of variance mutants compared with Δ36hENT3 at pH 7.4).

ther at pH 7.4 (Fig. 2*E*; estimated R of 0.11), suggesting His residues contribute minimally to pH sensing activity.

Dual mutation of Asp-219 and Glu-447 to Ala enables pH-independent activity to hENT3

To test the possibility of non-histidine-ionizable residues acting as the primary pH sensors of hENT3, we proceeded to investigate Asp and Glu, which can be protonated or deprotonated within a physiological pH range (Fig. 3*A*). Although the pK_a values of Asp and Glu (3.9 and 4.3, respectively) are below the functional pH range of hENT3, their actual pK_a could vary depending on their location within the protein structure (40, 41). To investigate the involvement of these amino acid residues, we again took an extensive alanine-scanning mutagenesis approach to generate mutants harboring Ala substitutions at a single position to abolish the negative charge. Of the 24 Asp and Glu mutants tested, Asp-to-Ala mutations at positions 156, 225, 279, 359, and 412 and Glu-to-Ala at positions 76 and 104 caused drastic reductions in [^{3}H]adenosine transport activity at pH 5.5 with no significant recovery of activity at 7.4 (Fig. 3*A*). These data identified the involvement of these five Asp and two Glu residues in the general transportability of hENT3 but ruled out any involvement in pH sensing. Intriguingly, Asp-to-Ala mutations at position 219 and Glu mutations to Ala at positions 95 and 447 recovered 5–8-fold higher transport activity at pH 7.4 when compared with that of Δ36hENT3 activity (Fig. 3*A*). These results suggested that the loss of a negative charge at any of these positions can enable hENT3 transportability at pH 7.4. Substantial retention of transport activities (≥60–70%) were also noted with these three mutants (D219A, E95A, and E447A) at pH 5.5, generating R values of ~0.64, 0.26, and 0.60, respectively (see Fig. 5*A*). An important distinction was that the transport magnitudes of all these three mutants at pH 7.4 (5–8-fold) were much higher than that of H268D and H473D mutations (2–4-fold), which opened up the possibility of one or more Asp/Glu residues, but not His, acting as primary pH sensors of hENT3.

To further confirm the role of Asp/Glu residues in pH-sensing, we made double and triple mutants of D219A, E95A, and E447A and determined whether any of those combinations can augment hENT3 transportability at pH 7.4. Intriguingly, the D219A/E447A double mutation maximally recovered hENT3 activity at pH 7.4 as well as observed at pH 5.5 (Fig. 3*B*) with an estimated R value of 0.98 (see Fig. 5*A*). However, the transport activity of double mutants D219A/E95A and E95A/E447A at pH 7.4 were lower than the D219A/E447A double mutant (R values of 0.46 and 0.44, respectively), indicating Glu-95 contributed only to a lesser extent than Asp-219 and Glu-447 in pH-sensing activity (Fig. 3*B* and see Fig. 5*A*). Therefore, the data thus far identified an estimated rank of Asp-219 > Glu-447 > Glu-95 > His-473 > His-268 for pH-sensing activity in hENT3. Consistent with maximal involvement of Asp-219 in the pH-sensing activity of hENT3, substitution of Ser-181 (a equivalent to Asp-219) to Asp in a pH-independent hENT2 partially con-

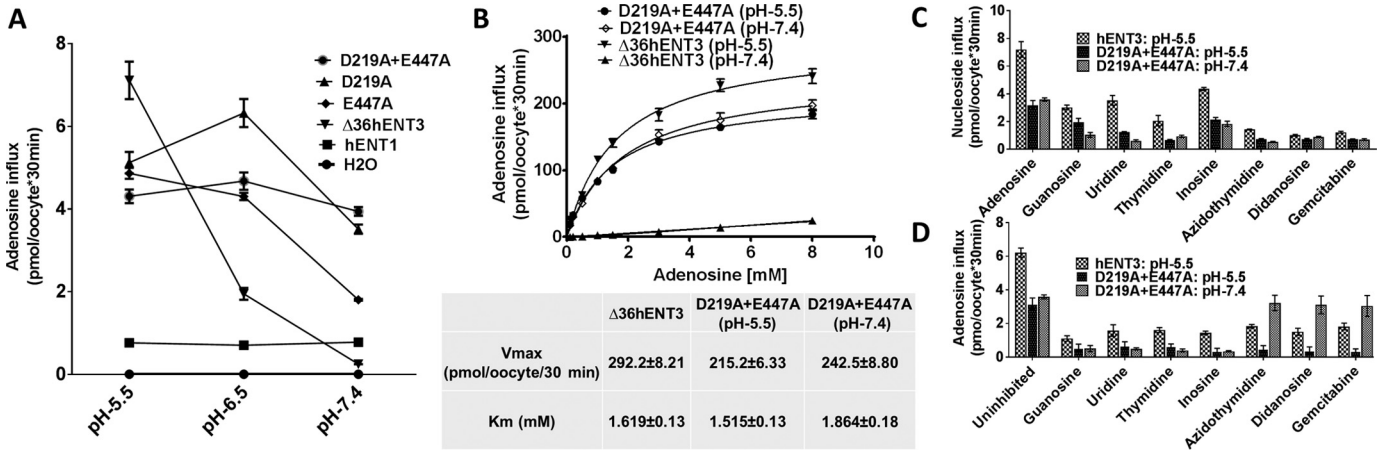

	Δ36hENT3	D219A+E447A (pH-5.5)	D219A+E447A (pH-7.4)
Vmax (pmol/oocyte/30 min)	292.2±8.21	215.2±6.33	242.5±8.80
Km (mM)	1.619±0.13	1.515±0.13	1.864±0.18

Figure 4. Verification of Asp-219 and Glu-447 as pH-sensing residues of hENT3. *A*, adenosine (20 μM) transport activities at different pH ranging from 4.5 to 8.5. *B*, transport activities of hENT3 and D219A and E447A double mutant at pH 5.5 and 7.4 against different adenosine concentrations. The V_{max} and K_m were calculated using Graphpad Prism. *C* and *D*, substrate selectively of hENT3 D219A and E447A double mutant. *C*, transport activities of different nucleosides and nucleoside drugs (20 μM) by hENT3 and D219A and E447A double mutant. *D*, transport activities of [^{3}H]adenosine (20 μM) by Δ36hENT3, and D219A/E447A double mutant transcript-injected *Xenopus* oocytes in the presence or absence of 1 mM concentration of various compounds at pH 5.5 (*C*) and 7.4 (*D*). Data show the average ± S.E. (n = 15–18 oocytes).

verted it into a pH-dependent transporter (R value decreased from 0.98 to 0.79) (supplemental Fig. S4).

Next, we also screened for possible contributions from cation-π interaction-capable group residues (Phe, Tyr, and Trp) and rare group residues (Ser, Thr, and Cys) toward pH sensing. Because there was a large number of these residues (17 Tyr, 29 Phe, 5 Trp, 53 Ser, 33 Thr, and 11 Cys) in hENT3, we only tested those residues that were conserved in its pH-sensitive paralog hENT4 and not in pH-independent paralogs hENT1 and hENT2. The mutation of Tyr to Ala at position 398 and Thr-to-Ala mutation at position 469 caused significantly decreased activity at pH 5.5, indicating their importance in general transportability of hENT3 (Fig. 3*C*). However, none of 13 Ala-substituted mutants in these categories, including Tyr-398 and Thr-469, demonstrated a significant increase in activity at pH 7.4, suggesting a lack of involvement of these residues in pH-sensing activities (Fig. 3*C*; see Fig. 5*A*). Moreover, these results further strengthened the role of Asp-219 and Glu-447 as the only major pH-sensing residues of hENT3 (see Fig. 5*A*).

To determine whether any other amino acid residues can replace the function of Asp-219 and Glu-447 in pH-sensing of hENT3, we substituted each of these two residues with numerous other amino acids and measured their transport activity. Interestingly, all substitutions contributed to pH-independent transport activity except for Cys substitution at position 219 (R value ~0.08) and Gln substitution at position 447 (R value ~0.16), which partially maintained pH-dependent activity (Fig. 3*D*). Cys is isosteric to Asp, and Gln is isosteric to Glu. Furthermore, both Cys and Gln are polar and capable of producing an electronegative pole depending on the pH of the environment (24). These facts suggest that the size and nature of amino acids at positions 219 and 447 are crucial for determining the acidic pH-dependent activity of hENT3.

Transport kinetics and substrate selectivity of D219A/E447A double mutant

To gain mechanistic insights into the role of Asp-219 and Glu-447 in pH-dependent activity of hENT3, we examined the transport features of D219A and E447A single mutants and the D219A/E447A double mutant. Contrary to Δ36hENT3, which showed a decline in [^{3}H]adenosine transport activity from pH 5.5 to 6.5 (Fig. 4*A*), the activity of the D219A mutant showed significantly increased transportability from pH 5.5 to 6.5 (Fig. 4*A*). Despite staying higher than that of Δ36hENT3, however, the transport activity of D219A mutant decreased at pH 7.4 when compared with its activity at pH 5.5 (Fig. 4*A*). These results suggest that the Asp-219 imparts a high, pH-restrictive activity within a narrow range of pH between 5.5 and 6.5. The transport activity of E447A mutant was the highest at pH 5.5 and only gradually decreased from pH 5.5 to 8.5. This is in sharp contrast to the steep decrease observed with that of Δ36hENT3 (Fig. 4*A*). These results suggest that Glu-447 exerts a low, pH-restrictive activity over a broad range of physiological pH ranges between 5.5 and 7.4. Interestingly, the transport activity of D219A/E447A double mutant largely remained the same in the entire range of acidic pH values tested (pH 5.5–7.0), demonstrating the D219A/E447A double mutant displayed functional activity closest to the pH-independent hENT1 transporter (Fig. 4*A*). Importantly, it also indicates that these two residues likely work in concert to bring an obligate acidic pH-dependent activity to hENT3.

We next analyzed for any alterations in the transport kinetics of the D219A/E447A double mutant (Fig. 4*B*). Although Δ36hENT3 transported adenosine at a K_m (apparent affinity) and V_{max} (maximal velocity) of 1.8 ± 0.12 mM and 292.2 ± 8.2 pmol/oocyte/30 min, respectively (10), the D219A/E447A double mutant exhibited a 27% decrease in the V_{max} (215.2 ± 6.3 pmol/oocyte/30 min) with a K_m of 1.5 ± 0.12 mM at pH 5.5 (Fig. 4*B*). Importantly, the transport profile of D219A/E447A double mutant at pH 7.4 largely resembled that of Δ36hENT3 at pH 5.5 with a V_{max} of 242.5 ± 8.8 pmol/oocyte/30 min (consistent with its R value of 0.98) and a K_m of 1.8 ± 0.18 mM. This indicated the affinity of the double mutant toward adenosine did not change appreciably with a change in pH. An analysis of the activity loss (calculated in V_{max}/K_m) showed that dual D219A and E447A

substitutions in hENT3 were associated with only a 1.27-fold decrease in activity at pH 5.5 but a >10-fold increase in activity at pH 7.4. This further corroborates the pH-independent function of the D219A/E447A double mutant.

Finally, we determined whether D219A/E447A double mutant exhibited any alterations in substrate selectivity. We tested the substrate and inhibitor characteristics of several endogenous nucleosides (guanosine, uridine, thymidine, and inosine) and therapeutic antiviral and anticancer nucleoside analogs (azidothymidine, didanosine, gemcitabine) that we reported earlier to interact with hENT3 (19). Similar to Δ36hENT3, the D219A/E447A double mutant maintained a stringent substrate selectivity for both endogenous nucleosides and nucleoside analogs at both pH 5.5 and 7.4, although the total transport fluxes were 20–30% lower than Δ36hENT3 (Fig. 4*C*) as expected from the reduced V_{max}/K_m for endogenous nucleoside (adenosine). Although the transportability of nucleoside analogs remained only subtly affected, the D219A/E447A double mutant escaped inhibition by the nucleoside analogs, *e.g.* azidothymidine, didanosine, and gemcitabine at pH 7.4 (Fig. 4*D*). Thus, our results identified the capability of D219A/E447A double mutant to transport nucleosides in a pH-independent fashion and suggest that the double mutant might have a slightly different conformation at 7.4 that prevents inhibition by some nucleoside analogs at higher concentrations.

Discussion

Human ENT3 is presumed to transport nucleosides across lysosomal membrane to support lysosomal metabolism and signaling. Consistently, gene deletion of hENT3 impairs lysosomal homeostasis (42). Independent research groups are increasingly reporting mutations in hENT3 as causing a spectrum of human genetic disorders including H syndrome, Faisalabad histiocytosis, SHML, PHID, RDD, and skeletal dystrophy (20–31). Despite this wide range of disorders resulting from exclusive mutation(s) in hENT3, the structural basis of hENT3 nucleoside transport remains unknown. Elucidation of hENT3 transport mechanism is likely to improve the understanding of cellular nucleoside transport characteristics, pathophysiology, and therapeutic interventions for hENT3 genetic disorders. The 475-residue hENT3 has 11 putative transmembrane domains, a large intracellular loop between TM6 and TM7, and a putative *N*-glycosylation site (43). The overall topology of hENT3 is very similar in all ENTs, except that hENT3 harbors an extended N terminus with hydrophilic domains harboring putative endosomal/lysosomal and mitochondrial targeting motifs (10). Truncation of the N terminus (Δ36NhENT3) redirects it from the intracellular domains to the cell surface allowing functional characterization of the transporter in *Xenopus* oocytes (10, 20). However, unlike hENT1 and hENT2, which shows maximum transport of nucleosides at pH 7.4, Δ36NhENT3 shows maximum transport only at an acidic pH of 5.5, consistent in its primary localization in lysosomes (10). The transport activity of hENT3 drops down drastically with the increasing pH range from 5.5 to 7.0 with only minimal activity retained at pH 7.4 (10). Experimental and phylogenetic analyses suggest that the pH-dependent nucleosides transport function is a conserved and early-evolved activity in two closely related members (hENT3 and hENT4) of the SLC29 family. The current study determined that hENT3 is a non-electrogenic transporter and that, depending on the pH of surrounding environment, the ionization states of Asp-219 and Glu-447 in hENT3 (which are predicted to be topologically located on the opposite sides of the lipid membrane) dictate the transport-permissible/impermissible conformations of hENT3 for nucleoside translocation.

Histidine switches are well known for regulating pH-dependent conformational changes of various enzymes and transporters (44–46). In addition, His switches are also known to play essential roles in pH-dependent substrate recognition, phospholipid-binding, and protein-protein interactions (45, 47, 48). However, contrary to our initial expectations, two His amino acids in hENT3 (His-268 and His-473) demonstrated only minimal pH-sensing activity, which lacked the robustness to transport nucleosides at pH 7.4 even when substituted with a positively charged Arg residue that mimicked protonated His at pH 7.4. Instead, systematical searching for other amino acid determinants of pH-dependent activity of hENT3 identified Asp-219, Glu-447, and Glu-95, in that order, to play prominent roles in regulating acidic pH-dependent activity. Asp-219 and Glu-447 locate to each half of the hENT3 transporter, and both residues are independently capable of exerting pH-restrictive activities at overlapping acidic pH ranges, regulating the opening and closing of the translocation pore at pH 5.5 and pH 7.4, respectively. Of all residues, Asp-219 exhibited the maximal transportability at pH 7.4 when replaced with non-ionizable residues. Intriguingly, hENT sequence alignments displayed Asp-219 as not present in either of the pH-independent hENT3 paralogs (hENT1 and hENT2) but conserved in several pH-dependent ENT3 orthologs (mouse, rat, and bovine; supplemental Fig. S2*A*). Substitution of an equivalent residue in hENT2 to Asp partially conferred pH-dependent activity to this otherwise pH-independent transporter. These findings lend credence for the primary role for Asp-219 in pH-sensing of acidic pH-driven ENT3 transporters from various species. Contrary to the mammalian orthologs, the yeast ortholog of hENT3 (FUN26) has an Ala (like hENT1) in place of Asp-219 of hENT3, which possibly explains the pH-independent function of the yeast transporter (supplemental Fig. S2*A*) (34). However, the Glu-447 residue is paradoxically conserved in all hENT3 paralogs and orthologs, the significance of which is at present unclear (supplemental Fig. S2, *A* and *B*). Nevertheless, Glu-447 is conserved in the *Arabidopsis* ENT1 protein, which is a proton-nucleoside cotransporter residing in the vacuolar membrane but not in six of eight other *Arabidopsis* isoforms.

In a lysosomal context, Asp-219 faces the lysosomal interior, and Glu-447 faces the cytosol (neutral milieu) (Fig. 5, *B* and *C*). In this scenario, the side chain of the Asp-219 became neutral in the acidic pH of the lysosomal interior, which energetically favored efflux of nucleosides out of lysosomes to cytosol, consistent with its fundamentally evolved function as a salvage protein to redirect preformed nucleosides for utilization into subsequent rounds of nucleic acid replication or as cofactors in biochemical pathways. Consistently, a homology 3D structure of hENT3 (predicted based on the structure of glycerol 3-phos-

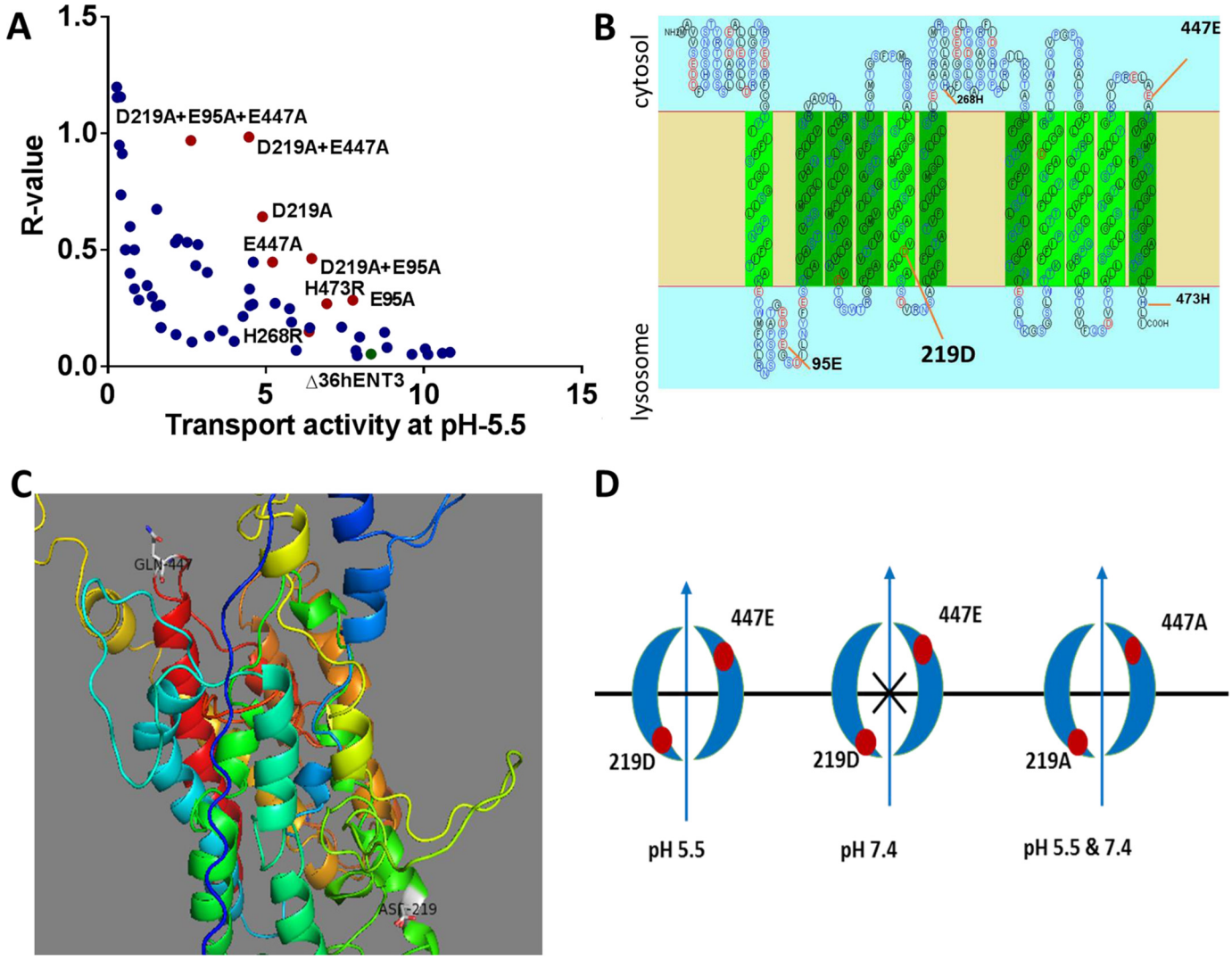

Figure 5. Proposed mechanism of hENT3 pH-dependent transport. *A*, R values of all mutants plotted against the transport activity at pH 5.5. *green dot*, Δ36hENT3; *red dots*, pH-independent mutants. *B*, topological structure of hENT3 indicating the location of pH sensor residues. *C*, 3D homology structure of hENT3 based on glycerol 3-phosphate transporter (Protein Data Bank code 1PW4). *D*, transport model of hENT3 in pH 5.5 and 7.4.

phate transporter in the Protein Data Bank with the highest Z-score among available crystal structure of proteins with hENT3, code 1PW4) revealed that the unionized side chain of Asp-219 at pH 5.5 does not interact with adjacent residues (particularly the Ala residue at position 230 where interaction occurs at pH 7.4) possibly allowing the opening of the nucleoside translocation pore (supplemental Fig. S3). Replacement of Asp-219 with a non-ionizable residue such as Ala completely abolished such interactions at both pH 5.5 and 7.4 (Fig. 5*D* and supplemental Fig. S3) and rendered transportability in a pH-independent fashion.

Conversely, Glu-447 is exposed to a steady cytosolic pH, and how a cytosolically located sensor works to measure lysosomal pH is currently unknown. There are several possibilities, however, for how this residue in ENT3 could act as an acidic pH sensor. First, the crystal structure of a CNT from *V. cholerae* shows that certain extracellular loops reenter the membrane as reentrant motifs (14). If an analogous situation exists in hENT3, Glu-447 in the cytosolic loop (only one residue away from being part of TMD 11) might reenter the membrane either interacting with the transport pore or even responding to any minor proton leaks through the transition pore. Based on the recent crystal structures of intermediate conformations of a CNT from *Neisseria wadsworthii* (49), it might also be possible that Glu-447 belongs to a scaffold domain in hENT3 that can come in contact with lysosomal protons when the nucleoside-binding transport domains make elevator-like transitions within the lipid membrane. Direct evidence for a cytoplasm-facing residue acting as pH sensor is also available from a bacterial arginine-agmatine antiporter, where a Tyr residue exposed to the stable cytosolic pH environment (not the periplasmic/extracellular side amenable to pH changes) serves as an intracellular gate (pH sensor) through cation-π interactions (33).

Unlike hENT3, transportability of hENT1 and hENT2 is generally tested at pH 7.4 with the ability of these transporters to function in subcellular organelle membranes (19, 32, 50) remaining obscure (where pH could differ from 7.4). Interestingly, our study brought to light the pH-independent function of hENT1 and hENT2, suggesting both are capable of transporting nucleosides at blood pH as well as in strong acidic

environments such as the late endosomes, lysosomes, luminal membrane of gastric epithelia, and tumor microenvironment (where ENTs are expressed at high levels). A recent study identified hENT1 mutations leading to abnormal ectopic mineralization of soft tissues in humans (51). Gene deletion of mouse ENT1 leads to progressive ectopic mineralization of spinal tissues resembling diffuse idiopathic skeletal hyperostosis in humans (51). Because osteoclastic activity depends on acidic pH and osteoclasts express high levels of hENT1, our current findings support a physiological role for hENT1 in osteoclast regulation.

Finally, our study also recognized several key amino acid residues (His-132, His-403, Asp-359, Asp-412, Glu-76, Glu-104, Glu-444, Tyr-398, Thr-469) necessary for the functional activity of hENT3 as mutations of these residues partially or fully disrupted transportability at pH 5.5. Because some of these residues are also mutated in hENT3 disorders (20), it would be of further interest to determine the precise role of these amino acids in substrate recognition, binding affinity, and membrane targeting to better understand hENT3 disorders. Furthermore, the identification of amino acid residues in hENT3 important in intracellular nucleoside transport and the lack of inhibition of Asp-219–Glu-447 double mutant to anti-HIV dideoxynucleosides at pH 7.4 may provide useful information for rational development of novel nucleoside analogs to potentially overcome clinical mitochondrial and/or lysosomal toxicities (19, 32).

Materials and methods

Materials and reagents

^{3}H radionucleotides were purchased from Moravek Radiochemicals (Brea, CA). Collagenase A was purchased from Roche Applied Science. Phenylmethanesulfonyl fluoride (PMSF), 4′,6′-diamidino-2-phenylindole (DAPI), uridine, adenosine, gentamycin, tricaine methanesulfonate, and other chemicals were purchased from Sigma. Fetal bovine serum (FBS) and horse serum were purchased from Corning Life Sciences. Penicillin-streptomycin and fluorescent antifade mounting reagent were obtained from Invitrogen. BCA protein assay reagent and SuperSignal™ West Pico Chemiluminescent substrate were obtained from Thermo Scientific. Taq polymerase, dNTPs, nuclease-free water, and restriction enzymes were purchased from Promega.

Plasmid constructs

pOX-hENT3 and pOX-Δ36hENT3 *Xenopus* expression constructs were described before (19, 20). The cDNA clones of hENT1, -2, and -4 were purchased from Dharmacon. The PCR products of hENT1, -2, and -4 were amplified using the following primers: hENT1 forward: 5′-GATTAGTCGACCCACCATGACAACCAGTCACCAG-3′; hENT1 reverse: 5′-GTATCTAGATCACACAATTGCCCG-3′; hENT2 forward: 5′-TTCAAGCTTCCACCATGGCGCGAGGAGACG-3′; hENT2 reverse: 5′-GTATCTAGATCAGAGCAGCGCCTTGAAGA-3′; hENT4 forward: 5′-TTAAAGCTTCCACCATGGGCTCCGTGGGGA-3′; hENT4 reverse: 5′-GTATCTAGATCAGAGGCCTGCGAGGATG-3′) and cloned into pOX vector using 5′SalI-3′XbaI, 5′HindIII-3′XbaI, and 5′HindIII-3′XbaI restriction sites, respectively. The plasmid constructs of hENT1, -2, and -4 were verified by Sanger sequencing in Georgia Genomic Facility and Ohio State Genomic Facility and named pOX-hENT1, pOX-hENT2, and pOX-hENT4, respectively.

Generation of mutant constructs

Point mutations were introduced into pOX-Δ36hENT3 construct using QuikChange® site-directed mutagenesis kit from Stratagene (La Jolla, CA) following the manufacturer's protocol. The HPLC grade mutagenic primers were purchased from IDT. The primers that were used to make single-point mutations and combinations of point mutations are listed in supplemental Table S1. The mutant plasmids were purified using E.Z.N.A.TM plasmid mini prep kit I (Omega Bio-Tek, Norcross, GA) and verified by Sanger sequencing in Georgia Genomic Facility and Ohio State Genomic Facility.

In vitro transcription and expression in Xenopus oocytes

The mutant plasmids were linearized by either Not1 or Sac1 restriction enzyme. The digested products were purified by phenol-chloroform extraction. The mRNAs were synthesized using mMESSAGE mMACHINE (Ambion) transcription kits following the manufacturer's instructions. The mRNAs were purified by the lithium precipitation method. Fifty nanoliters (400–800 ng/μl) of equal amounts of mRNAs were injected into defolliculated oocytes the next day. The injected oocytes were incubated at 15 °C for 24 h before performing transport assays. Uptake of radiolabeled substrates was measured after 30 min of incubation in transport buffer (100 mM NaCl, 2 mM KCl, 1 mM $CaCl_2$, 1 mM $MgCl_2$, and 10 mM HEPES, pH 7.4) at room temperature. Uptake was terminated by washing oocytes 3 times with arrest buffer (20 mM Tris-HCl, 3 mM K_2HPO_4, 1 mM $MgCl_2{\cdot}6H_2O$, 2 mM $CaCl_2$, 5 mM glucose, 130 mM *N*-methyl-D-glucamine) containing 20 mM uridine. Individual oocytes were shaken overnight in 10% SDS for complete dissolution, and then the radioactivity was quantified by Beckman liquid scintillation counter. Data represent the average ± S.E. (n = 8–20 oocytes). A representative experiment from 3–5 independent experiments is presented.

Electrophysiological assessment in Xenopus oocytes

A two-electrode voltage clamp was used to measure whole-cell macroscopic currents (36, 37, 52). Oocytes were bathed in solution containing transport buffer (100 mM NaCl, 2 mM KCl, 1 mM $CaCl_2$, 1 mM $MgCl_2$, and 10 mM HEPES) at pH 7.4 (hCNT2 recordings) or 5.5 (water injected and Δ36hENT3). Glass electrodes (1–2.5-megaohm resistance) were pulled with a Sutter P-97 micropipette puller (Sutter Instrument Co., Novato, CA) and filled with 3 M KCl. Data were recorded at room temperature using a Clamp OC-725 Amplifier (Warner Instruments, Hamden, CT) and a Powerlab 4SP digitizer with CHART software (ADInstruments). Oocytes were held at −50 mV, and only data from oocytes with an initial resting membrane potential of −30 mV or below were analyzed. Adenosine was applied at a concentration of 100 μM, and adenosine-evoked currents were quantified by determining the average current amplitude 5–15 s after adenosine addition. Data were

compiled from the adenosine response from at least eight oocytes.

Homology modeling

Glycerol 3-phosphate transporter (Protein Data Bank code 1PW4) with the highest Z-score among available crystal structures of proteins with hENT3 was used as the structural template for developing the models as shown earlier (20). The model was developed using Modeler through Chimera interface (53, 54).

Author contributions—R. G. and F. R. conceived and designed the study. F. R. designed and constructed the vectors for expression of mutant proteins, analyzed the mutant phenotypes in Xenopus oocytes, and conducted the homology modeling analysis. C. A. conducted and interpreted electrophysiological experiments. All authors analyzed the results, wrote the paper, and approved the final version of the manuscript.

References

1. Baldwin, S. A., Beal, P. R., Yao, S. Y., King, A. E., Cass, C. E., and Young, J. D. (2004) The equilibrative nucleoside transporter family, SLC29. *Pflugers Arch.* **447,** 735–743
2. Gray, J. H., Owen, R. P., and Giacomini, K. M. (2004) The concentrative nucleoside transporter family, SLC28. *Pflugers Arch.* **447,** 728–734
3. Young, J. D., Yao, S. Y., Sun, L., Cass, C. E., and Baldwin, S. A. (2008) Human equilibrative nucleoside transporter (ENT) family of nucleoside and nucleobase transporter proteins. *Xenobiotica* **38,** 995–1021
4. Pastor-Anglada, M., Cano-Soldado, P., Errasti-Murugarren, E., and Casado, F. J. (2008) SLC28 genes and concentrative nucleoside transporter (CNT) proteins. *Xenobiotica* **38,** 972–994
5. Felipe, A., Valdes, R., Santo, B., Lloberas, J., Casado, J., and Pastor-Anglada, M. (1998) Na^+-dependent nucleoside transport in liver: two different isoforms from the same gene family are expressed in liver cells. *Biochem. J.* **330,** 997–1001
6. Ngo, L. Y., Patil, S. D., and Unadkat, J. D. (2001) Ontogenic and longitudinal activity of Na^+-nucleoside transporters in the human intestine. *Am. J. Physiol. Gastrointest. Liver Physiol.* **280,** G475–G481
7. Pennycooke, M., Chaudary, N., Shuralyova, I., Zhang, Y., and Coe, I. R. (2001) Differential expression of human nucleoside transporters in normal and tumor tissue. *Biochem. Biophys. Res. Commun.* **280,** 951–959
8. Ritzel, M. W., Yao, S. Y., Huang, M. Y., Elliott, J. F., Cass, C. E., and Young, J. D. (1997) Molecular cloning and functional expression of cDNAs encoding a human Na^+-nucleoside cotransporter (hCNT1). *Am. J. Physiol.* **272,** C707–C714
9. Govindarajan, R., Bakken, A. H., Hudkins, K. L., Lai, Y., Casado, F. J., Pastor-Anglada, M., Tse, C. M., Hayashi, J., and Unadkat, J. D. (2007) In situ hybridization and immunolocalization of concentrative and equilibrative nucleoside transporters in the human intestine, liver, kidneys, and placenta. *Am. J. Physiol. Regul. Integr. Comp. Physiol.* **293,** R1809–R1822
10. Baldwin, S. A., Yao, S. Y., Hyde, R. J., Ng, A. M., Foppolo, S., Barnes, K., Ritzel, M. W., Cass, C. E., and Young, J. D. (2005) Functional characterization of novel human and mouse equilibrative nucleoside transporters (hENT3 and mENT3) located in intracellular membranes. *J. Biol. Chem.* **280,** 15880–15887
11. Cano-Soldado, P., Gorraitz, E., Errasti-Murugarren, E., Casado, F. J., Lostao, M. P., and Pastor-Anglada, M. (2012) Functional analysis of the human concentrative nucleoside transporter-1 variant hCNT1S546P provides insight into the sodium-binding pocket. *Am. J. Physiol. Cell Physiol.* **302,** C257–C266
12. Slugoski, M. D., Ng, A. M., Yao, S. Y., Smith, K. M., Lin, C. C., Zhang, J., Karpinski, E., Cass, C. E., Baldwin, S. A., and Young, J. D. (2008) A proton-mediated conformational shift identifies a mobile pore-lining cysteine residue (Cys-561) in human concentrative nucleoside transporter 3. *J. Biol. Chem.* **283,** 8496–8507
13. Slugoski, M. D., Ng, A. M., Yao, S. Y., Lin, C. C., Mulinta, R., Cass, C. E., Baldwin, S. A., and Young, J. D. (2009) Substituted cysteine accessibility method analysis of human concentrative nucleoside transporter hCNT3 reveals a novel discontinuous region of functional importance within the CNT family motif (G/A)*XKX*3NEFVA(Y/M/F). *J. Biol. Chem.* **284,** 17281–17292
14. Johnson, Z. L., Cheong, C. G., and Lee, S. Y. (2012) Crystal structure of a concentrative nucleoside transporter from *Vibrio cholerae* at 2.4 Å. *Nature* **483,** 489–493
15. Endres, C. J., and Unadkat, J. D. (2005) Residues Met89 and Ser160 in the human equilibrative nucleoside transporter 1 affect its affinity for adenosine, guanosine, S6-(4-nitrobenzyl)-mercaptopurine riboside, and dipyridamole. *Mol. Pharmacol.* **67,** 837–844
16. Visser, F., Vickers, M. F., Ng, A. M., Baldwin, S. A., Young, J. D., and Cass, C. E. (2002) Mutation of residue 33 of human equilibrative nucleoside transporters 1 and 2 alters sensitivity to inhibition of transport by dilazep and dipyridamole. *J. Biol. Chem.* **277,** 395–401
17. Visser, F., Sun, L., Damaraju, V., Tackaberry, T., Peng, Y., Robins, M. J., Baldwin, S. A., Young, J. D., and Cass, C. E. (2007) Residues 334 and 338 in transmembrane segment 8 of human equilibrative nucleoside transporter 1 are important determinants of inhibitor sensitivity, protein folding, and catalytic turnover. *J. Biol. Chem.* **282,** 14148–14157
18. Barnes, K., Dobrzynski, H., Foppolo, S., Beal, P. R., Ismat, F., Scullion, E. R., Sun, L., Tellez, J., Ritzel, M. W., Claycomb, W. C., Cass, C. E., Young, J. D., Billeter-Clark, R., Boyett, M. R., and Baldwin, S. A. (2006) Distribution and functional characterization of equilibrative nucleoside transporter-4, a novel cardiac adenosine transporter activated at acidic pH. *Circ. Res.* **99,** 510–519
19. Govindarajan, R., Leung, G. P., Zhou, M., Tse, C. M., Wang, J., and Unadkat, J. D. (2009) Facilitated mitochondrial import of antiviral and anticancer nucleoside drugs by human equilibrative nucleoside transporter-3. *Am. J. Physiol. Gastrointest. Liver Physiol.* **296,** G910–G922
20. Kang, N., Jun, A. H., Bhutia, Y. D., Kannan, N., Unadkat, J. D., and Govindarajan, R. (2010) Human equilibrative nucleoside transporter-3 (hENT3) spectrum disorder mutations impair nucleoside transport, protein localization, and stability. *J. Biol. Chem.* **285,** 28343–28352
21. Morgan, N. V., Morris, M. R., Cangul, H., Gleeson, D., Straatman-Iwanowska, A., Davies, N., Keenan, S., Pasha, S., Rahman, F., Gentle, D., Vreeswijk, M. P., Devilee, P., Knowles, M. A., Ceylaner, S., Trembath, R. C., Dalence, C., *et al.* (2010) Mutations in SLC29A3, encoding an equilibrative nucleoside transporter ENT3, cause a familial histiocytosis syndrome (Faisalabad histiocytosis) and familial Rosai-Dorfman disease. *PLoS Genet.* **6,** e1000833
22. Molho-Pessach, V., Lerer, I., Abeliovich, D., Agha, Z., Abu Libdeh, A., Broshtilova, V., Elpeleg, O., and Zlotogorski, A. (2008) The H syndrome is caused by mutations in the nucleoside transporter hENT3. *Am. J. Hum. Genet.* **83,** 529–534
23. Campeau, P. M., Lu, J. T., Sule, G., Jiang, M. M., Bae, Y., Madan, S., Högler, W., Shaw, N. J., Mumm, S., Gibbs, R. A., Whyte, M. P., and Lee, B. H. (2012) Whole-exome sequencing identifies mutations in the nucleoside transporter gene SLC29A3 in dysosteosclerosis, a form of osteopetrosis. *Hum. Mol. Genet.* **21,** 4904–4909
24. Cliffe, S. T., Kramer, J. M., Hussain, K., Robben, J. H., de Jong, E. K., de Brouwer, A. P., Nibbeling, E., Kamsteeg, E. J., Wong, M., Prendiville, J., James, C., Padidela, R., Becknell, C., van Bokhoven, H., Deen, P. M., *et al.* (2009) SLC29A3 gene is mutated in pigmented hypertrichosis with insulin-dependent diabetes mellitus syndrome and interacts with the insulin signaling pathway. *Hum. Mol. Genet.* **18,** 2257–2265
25. Priya, T. P., Philip, N., Molho-Pessach, V., Busa, T., Dalal, A., and Zlotogorski, A. (2010) H syndrome: novel and recurrent mutations in SLC29A3. *Br. J. Dermatol.* **162,** 1132–1134
26. Ramot, Y., Sayama, K., Sheffer, R., Doviner, V., Hiller, N., Kaufmann-Yehezkely, M., and Zlotogorski, A. (2010) Early-onset sensorineural hearing loss is a prominent feature of H syndrome. *Int. J. Pediatr. Otorhinolaryngol.* **74,** 825–827
27. Colmenero, I., Molho-Pessach, V., Torrelo, A., Zlotogorski, A., and Requena, L. (2012) Emperipolesis: an additional common histopathologic

finding in H syndrome and Rosai-Dorfman disease. *Am. J. Dermatopathol.* **34,** 315–320
28. Farooq, M., Moustafa, R. M., Fujimoto, A., Fujikawa, H., Abbas, O., Kibbi, A. G., Kurban, M., and Shimomura, Y. (2012) Identification of two novel mutations in SLC29A3 encoding an equilibrative nucleoside transporter (hENT3) in two distinct Syrian families with H syndrome: expression studies of SLC29A3 (hENT3) in human skin. *Dermatology* **224,** 277–284
29. de Jesus, J., Imane, Z., Senée, V., Romero, S., Guillausseau, P. J., Balafrej, A., and Julier, C. (2013) SLC29A3 mutation in a patient with syndromic diabetes with features of pigmented hypertrichotic dermatosis with insulin-dependent diabetes, H syndrome and Faisalabad histiocytosis. *Diabetes Metab.* **39,** 281–285
30. Elbarbary, N. S., Tjora, E., Molnes, J., Lie, B. A., Habib, M. A., Salem, M. A., and Njølstad, P. R. (2013) An Egyptian family with H syndrome due to a novel mutation in SLC29A3 illustrating overlapping features with pigmented hypertrichotic dermatosis with insulin-dependent diabetes and Faisalabad histiocytosis. *Pediatr. Diabetes* **14,** 466–472
31. Al-Haggar, M., Salem, N., Wahba, Y., Ahmad, N., Jonard, L., Abdel-Hady, D., El-Hawary, A., El-Sharkawy, A., Eid, A. R., and El-Hawary, A. (2015) Novel homozygous SLC29A3 mutations among two unrelated Egyptian families with spectral features of H-syndrome. *Pediatr. Diabetes* **16,** 305–316
32. Lee, E. W., Lai, Y., Zhang, H., and Unadkat, J. D. (2006) Identification of the mitochondrial targeting signal of the human equilibrative nucleoside transporter 1 (hENT1): implications for interspecies differences in mitochondrial toxicity of fialuridine. *J. Biol. Chem.* **281,** 16700–16706
33. Wang, S., Yan, R., Zhang, X., Chu, Q., and Shi, Y. (2014) Molecular mechanism of pH-dependent substrate transport by an arginine-agmatine antiporter. *Proc. Natl. Acad. Sci. U.S.A.* **111,** 12734–12739
34. Boswell-Casteel, R. C., Johnson, J. M., Duggan, K. D., Roe-Žurž, Z., Schmitz, H., Burleson, C., and Hays, F. A. (2014) FUN26 (function unknown now 26) protein from saccharomyces cerevisiae is a broad selectivity, high affinity, nucleoside and nucleobase transporter. *J. Biol. Chem.* **289,** 24440–24451
35. Young, J. D., Yao, S. Y., Baldwin, J. M., Cass, C. E., and Baldwin, S. A. (2013) The human concentrative and equilibrative nucleoside transporter families, SLC28 and SLC29. *Mol. Aspects Med.* **34,** 529–547
36. Larráyoz, I. M., Fernández-Nistal, A., Garcés, A., Gorraitz, E., and Lostao, M. P. (2006) Characterization of the rat Na^+/nucleoside cotransporter 2 and transport of nucleoside-derived drugs using electrophysiological methods. *Am. J. Physiol. Cell Physiol.* **291,** C1395–C1404
37. Smith, K. M., Ng, A. M., Yao, S. Y., Labedz, K. A., Knaus, E. E., Wiebe, L. I., Cass, C. E., Baldwin, S. A., Chen, X. Z., Karpinski, E., and Young, J. D. (2004) Electrophysiological characterization of a recombinant human Na^+-coupled nucleoside transporter (hCNT1) produced in *Xenopus* oocytes. *J. Physiol.* **558,** 807–823
38. Gallivan, J. P., and Dougherty, D. A. (1999) Cation-π interactions in structural biology. *Proc. Natl. Acad. Sci. U.S.A.* **96,** 9459–9464
39. Dougherty, D. A. (2007) Cation-π interactions involving aromatic amino acids. *J. Nutr.* **137,** 1504S–1508S; discussion 1516S–1517S
40. Di Russo, N. V., Estrin, D. A., Martí, M. A., and Roitberg, A. E. (2012) pH-Dependent conformational changes in proteins and their effect on experimental pK_as: the case of Nitrophorin 4. *PLoS Comput. Biol.* **8,** e1002761
41. Stennicke, H. R., Mortensen, U. H., Christensen, U., Remington, S. J., and Breddam, K. (1994) Effects of introduced aspartic and glutamic acid residues on the P′1 substrate specificity, pH dependence and stability of carboxypeptidase Y. *Protein Eng.* **7,** 911–916
42. Hsu, C. L., Lin, W., Seshasayee, D., Chen, Y. H., Ding, X., Lin, Z., Suto, E., Huang, Z., Lee, W. P., Park, H., Xu, M., Sun, M., Rangell, L., Lutman, J. L., Ulufatu, S., Stefanich, E., *et al.* (2012) Equilibrative nucleoside transporter 3 deficiency perturbs lysosome function and macrophage homeostasis. *Science* **335,** 89–92
43. Hyde, R. J., Cass, C. E., Young, J. D., and Baldwin, S. A. (2001) The ENT family of eukaryote nucleoside and nucleobase transporters: recent advances in the investigation of structure/function relationships and the identification of novel isoforms. *Mol. Membr. Biol.* **18,** 53–63
44. Mueller, D. S., Kampmann, T., Yennamalli, R., Young, P. R., Kobe, B., and Mark, A. E. (2008) Histidine protonation and the activation of viral fusion proteins. *Biochem. Soc. Trans.* **36,** 43–45
45. Rötzschke, O., Lau, J. M., Hofstätter, M., Falk, K., and Strominger, J. L. (2002) A pH-sensitive histidine residue as control element for ligand release from HLA-DR molecules. *Proc. Natl. Acad. Sci. U.S.A.* **99,** 16946–16950
46. Achilonu, I., Fanucchi, S., Cross, M., Fernandes, M., and Dirr, H. W. (2012) Role of individual histidines in the pH-dependent global stability of human chloride intracellular channel 1. *Biochemistry* **51,** 995–1004
47. Cauët, E., Rooman, M., Wintjens, R., Liévin, J., and Biot, C. (2005) Histidine-aromatic interactions in proteins and protein-ligand complexes: quantum chemical study of X-ray and model structures. *J. Chem. Theory Comput.* **1,** 472–483
48. Ames, G. F., and Spurich, E. N. (1976) Protein-protein interaction in transport: periplasmic histidine-binding protein J interacts with P protein. *Proc. Natl. Acad. Sci. U.S.A.* **73,** 1877–1881
49. Hirschi, M., Johnson, Z. L., and Lee, S. Y. (2017) Visualizing multistep elevator-like transitions of a nucleoside transporter. *Nature* **545,** 66–70
50. Mangravite, L. M., Xiao, G., and Giacomini, K. M. (2003) Localization of human equilibrative nucleoside transporters, hENT1 and hENT2, in renal epithelial cells. *Am. J. Physiol. Renal Physiol.* **284,** F902–F910
51. Warraich, S., Bone, D. B., Quinonez, D., Ii, H., Choi, D. S., Holdsworth, D. W., Drangova, M., Dixon, S. J., Séguin, C. A., and Hammond, J. R. (2013) Loss of equilibrative nucleoside transporter 1 in mice leads to progressive ectopic mineralization of spinal tissues resembling diffuse idiopathic skeletal hyperostosis in humans. *J. Bone Miner. Res.* **28,** 1135–1149
52. Frey, E. N., Pavlovicz, R. E., Wegman, C. J., Li, C., and Askwith, C. C. (2013) Conformational changes in the lower palm domain of ASIC1a contribute to desensitization and RFamide modulation. *PLoS ONE* **8,** e71733
53. Sali, A., and Blundell, T. L. (1993) Comparative protein modelling by satisfaction of spatial restraints. *J. Mol. Biol.* **234,** 779–815
54. Pettersen, E. F., Goddard, T. D., Huang, C. C., Couch, G. S., Greenblatt, D. M., Meng, E. C., and Ferrin, T. E. (2004) UCSF Chimera–a visualization system for exploratory research and analysis. *J. Comput. Chem.* **25,** 1605–1612